Phase transition peculiarities in LAMOX single crystals

# Phase transition peculiarities in LAMOX single crystals

## V I Voronkova[1], E P Kharitonova[1], A E Krasilnikova[1] and N N Kononkova[2]

[1] Faculty of Physics, M V Lomonosov Moscow State University, Leninskie Gory, Russia
[2] Vernadsky Institute of Geochemistry and Analytical Chemistry, Russian Academy of Sciences, Moscow, Russia

E-mail: voronk@polly.phys.msu.ru

## Abstract

The series of oxide-ion-conducting $La_2Mo_2O_9$ single crystals, undoped and doped with Ca, Bi, W, Nb, Zn and V (LAMOX), was grown by the flux method in the system $La_2O_3$–$MoO_3$, which has allowed us to use polarization microscopy for the identification of phases. Phase transition peculiarities in the LAMOX family have been studied by polarization microscopy and calorimetry. The results demonstrate that both the monoclinic phase ($\alpha$), which is stable at room temperature, and the metastable cubic phase ($\beta_{ms}$), or a mixture of these phases, may exist at room temperature, depending on the post-growth cooling rate and the nature of the dopant at low doping level. On heating, all of the quenched crystals undergo $\beta_{ms} \rightarrow \alpha$ (450 °C) and $\alpha \rightarrow \beta$ (500–560 °C) phase transitions (where $\beta$ designates the stable cubic phase). At heavy doping levels, the high-temperature transition is suppressed and the crystals ($La_2Mo_{1.95}V_{0.05}O_y$, $La_2Mo_{1.84}W_{0.16}O_y$ in our case) are found in the cubic state. The thermal peak near 450 °C at high doping level is not associated with a $\beta_{ms} \rightarrow \alpha$ transition and may be the result of defect association/dissociation in the cubic crystals. The thermal history, nature of the dopant and doping level are shown to influence the phase transition sequence and type.

## 1. Introduction

The LAMOX family of fast oxide-ion conductors, first discovered in 2000, based on lanthanum molybdate (LM), $La_2Mo_2O_9$, doped with various cations, has recently attracted a great deal of attention as a source of solid electrolytes for advanced energy technologies [1]. Near 580 °C, $La_2Mo_2O_9$ undergoes a first-order phase transition to a superionic, disordered state, which shows up both in electrical conductivity measurements (as a conductivity jump by two orders of magnitude, to $6 \times 10^{-2}$ S cm$^{-1}$) and in studies of the thermal properties of LM by differential thermal analysis (DTA), high-temperature x-ray diffraction (XRD) and dilatometry [1, 2]. The DTA curve of LM shows an endothermic peak near 580 °C during heating and an exothermic peak at a 40 °C lower temperature during cooling.

According to Goutenoire *et al* [3], LM has a monoclinic structure (space group $P2_1$) at low temperatures ($\alpha$-phase) and a cubic structure (space group $P2_13$) at high temperatures ($\beta$-phase). The structure of the high-temperature phase was

reported in [3]. Its unit-cell parameter was determined to be $a = 7.20$ Å at 617 °C. The low-temperature phase has a complex structure, with a $2a \times 3a \times 4a$ superstructure, which appears pseudo-cubic, with $a = 7.15$ Å according to room-temperature XRD data [3]. XRD of the phases $\alpha$ and $\beta$ are practically identical, because the structural phase transition $\alpha \rightarrow \beta$ is actually a transition from a static to dynamic distribution of the oxygen defects without any shift of heavy atoms [4]. Only high-resolution XRD is required for revealing the monoclinic $\alpha$-phase. The structure of the $\alpha$-phase was solved only in 2005 by Evans *et al* [5] and was shown to comprise a large number of nonequivalent atoms: 48 La, 48 Mo and 216 O. This complex structure of the monoclinic phase impedes the oxygen ordering underlying the $\beta \rightarrow \alpha$ phase transition. It was established that the domains have been observed in single crystals of the monoclinic phase [6].

According to a number of reports [7–14], many dopants substituting for lanthanum (K, Ca, Sr, Ba, Bi, Y, Sm, Gd, Dy, Er) or molybdenum (V, W, Cr) suppress the $\beta \rightarrow \alpha$ phase transition, enabling the cubic phase to persist metastably at

**Table 1.** Initial melt compositions, crystal compositions (chemical analysis data) and unit-cell parameters.

| Initial melt compositions (mol%) | | | | Unit-cell parameters, (Å) |
|---|---|---|---|---|
| $La_2O_3$ | $MoO_3$ | Me-oxide | Crystal compositions | |
| 29 | 71 | — | $La_2Mo_2O_9$ | 7.164 |
| 29 | 71 | $2CaO$ | $La_{1.96}Ca_{0.04}Mo_2O_y$ | 7.156 |
| 29 | 71 | $2Bi_2O_3$ | $La_{1.96}Bi_{0.04}Mo_2O_y$ | 7.166 |
| 29 | 71 | $1WO_3$ | $La_2Mo_{1.92}W_{0.08}O_y$ | 7.158 |
| 29 | 71 | $2WO_3$ | $La_2Mo_{1.84}W_{0.16}O_y$ | 7.158 |
| 29 | 71 | $0.25Nb_2O_5$ | $La_2Mo_{1.98}Nb_{0.02}O_y$ | 7.159 |
| 29 | 71 | $1ZnO$ | $La_2Mo_{1.95}Zn_{0.05}O_y$ | 7.160 |
| 29 | 71 | $1V_2O_5$ | $La_2Mo_{1.95}V_{0.05}O_y$ | 7.154 |

all temperature ranges. At the same time, Al, Fe, Mn and Nb substitutions on the Mo site have an insignificant effect on the phase transition [13]. Moreover, whether the low- or high-temperature phase exists at room temperature depends on the cooling rate of the synthesized samples and doping level. So, in a number of works [6, 14, 15] the metastable cubic state of the phase at room temperature was revealed later on sample quenching, and the transition from metastable $\beta_{ms}$-phase in the $\alpha$-phase was observed at the temperature $420\,^\circ$C (high-temperature x-ray) in [14]. Quenched LM single crystals were reported to have a cubic structure, whereas slow cooling, at a rate of the order of 1 K min$^{-1}$, leads to the formation of the low-temperature, monoclinic phase [6].
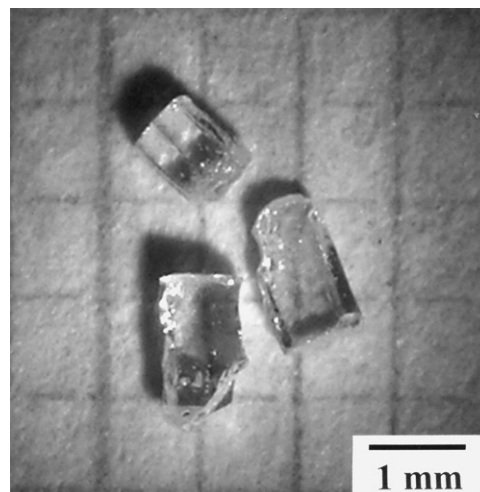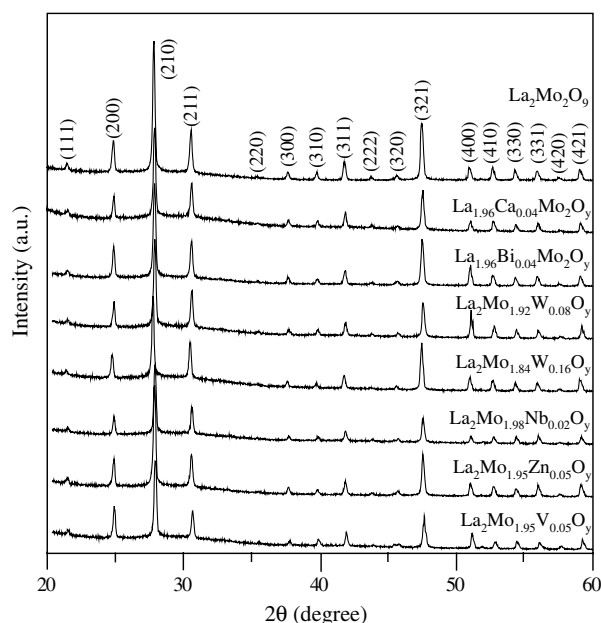
In this paper, we report the first detailed study of the phase transition peculiarities in undoped and doped (Ca, Bi, Nb, V, W and Zn) LM single crystals depending on the dopant nature and content and on the thermal history of the single crystals by polarization microscopy and calorimetry.

## 2. Experimental details

Crystals for this investigation were grown from off-stoichiometric melts and were then quenched or furnace-cooled at a rate of the order of 1 K min$^{-1}$. The $La_2O_3$:$MoO_3$ molar ratio in the melts was 29:71, and the dopants used were $CaO$, $Bi_2O_3$, $Nb_2O_5$, $V_2O_5$, $WO_3$ and $ZnO$. The crystals were obtained the first time. The compositions of the melts and the grown crystals are listed in table 1. The crystal growth procedure was described in detail elsewhere [6].

The quenched crystals were furnace-annealed at 100, 200, 300, 400, 450 and 500 $^\circ$C for 2 h and were then examined under an MIN-8 polarization microscope equipped with a high-temperature stage.

The crystals identification was made by XRD on a DRON-2.0 diffractometer with Cu K$\alpha$ radiation. The scans were performed in the $2\theta$ range (20–60$^\circ$) with 0.02$^\circ$ step. The thermal behaviour of the crystals was studied by differential scanning calorimetry (DSC) and thermal analysis in air, using NETZSCH DSC 204 F1 and STA 449 C instruments. The heating/cooling rate was 10 K min$^{-1}$. The results obtained with the two instruments differed insignificantly. The samples were, as a rule, equilibrated by two to five heating/cooling cycles. Dielectric permittivity was measured from 25 to 700 $^\circ$C at 1 MHz using a Tesla BM 431E bridge. The chemical



**Figure 1.** $La_2Mo_2O_9$ single crystals grown in the system $La_2O_3$–$MoO_3$.



**Figure 2.** The XRD patterns of pure and doped $La_2Mo_2O_9$ ground single crystals.

composition of the crystals was determined on a CAMEBAX SX-50 microanalyser with an accuracy of $\pm 0.02$ mass%.

## 3. Results and discussion

The undoped and doped LM single crystals grown as described above were 1–4 mm in size (figure 1). The XRD patterns of pure and doped $La_2Mo_2O_9$ ground crystals are shown in figure 2. The XRD patterns of the doped crystals were identical with the $La_2Mo_2O_9$ pattern and with the data of Fournier *et al* [16]. The crystals were identified as pseudo-cubic with the unit-cell parameters listed in table 1.

The phase transformations in the quenched and slowly cooled single crystals were investigated by polarization
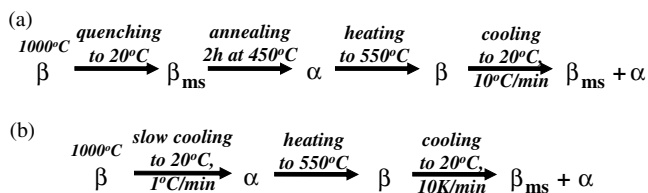
(a)

$$1000^{o}C \xrightarrow[\text{to } 20^{o}C]{\textit{quenching}} \beta_{\mathbf{ms}} \xrightarrow[\text{2h at } 450^{o}C]{\textit{annealing}} \alpha \xrightarrow[\text{to } 550^{o}C]{\textit{heating}} \beta \xrightarrow[\text{10}^{o}C/min]{\textit{cooling}} \beta_{\mathbf{ms}} + \alpha$$

(b)

$$1000^{o}C \xrightarrow[\text{1}^{o}C/min]{\textit{slow cooling}} \alpha \xrightarrow[\text{to } 550^{o}C]{\textit{heating}} \beta \xrightarrow[\text{10K/min}]{\textit{cooling}} \beta_{\mathbf{ms}} + \alpha$$

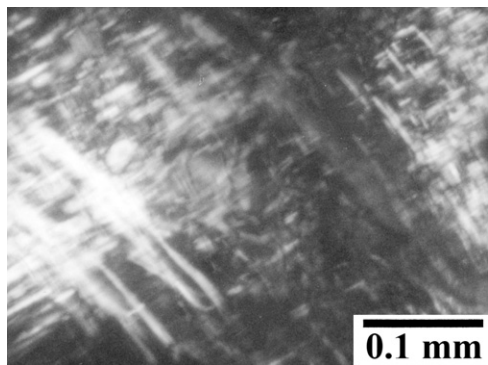**Figure 3.** The phase transformation scheme of (a) quenched and (b) slowly cooled $La_2Mo_2O_9$ single crystals.



**Figure 4.** Microphotograph of the $La_2Mo_2O_9$ domain structure.

microscopy. The results are represented schematically in figure 3. At room temperature, the quenched crystals were isotropic, suggesting that the cubic phase persisted metastably (this phase will be designated $\beta_{ms}$). Moreover, the metastable cubic phase persisted during heating from 100 to 400 °C, whereas annealing near 450 °C resulted in a transition to the monoclinic, anisotropic phase ($\alpha$) and the formation of domains (figure 4). Therefore, under the conditions of this study, the temperature of the transition from the metastable cubic phase ($\beta_{ms}$) to the monoclinic phase ($\alpha$) is of the order of 450 °C. Heating to about 550 °C led to the formation of the stable cubic phase ($\beta$), at the same time domains disappeared and the phase became isotropic. After subsequent cooling to room temperature at a rate of 10 K min$^{-1}$, the crystals consisted of the $\beta_{ms}$-phase (isotropic) and a small amount of the $\alpha$-phase (anisotropic), indicating that cooling at 10 K min$^{-1}$ was too slow for the formation of a pure $\beta_{ms}$-phase and too rapid for the formation of the $\alpha$-phase.

The slowly cooled (1 K min$^{-1}$) crystals (figure 4) were anisotropic and were composed of many mutually perpendicular domains, characteristic of the $\alpha$-phase [6]. At 550 °C, the stable cubic phase was formed. During subsequent cooling at 10 K min$^{-1}$, the cubic phase did not fully convert to the stable $\beta$-phase, and the crystals were two-phase at room temperature, like the quenched crystals. It follows from the above that the $\beta_{ms}$-phase can be eliminated by annealing near 450 °C; the annealed crystals then consist of the $\alpha$-phase, which is stable at room temperature.

Note that the above scheme of phase transformations in LAMOX crystals does not apply to $La_2Mo_{1.95}V_{0.05}O_y$ and $La_2Mo_{1.84}W_{0.16}O_y$, which have a cubic structure at any temperature, with the $\beta \to \alpha$ phase transition suppressed.

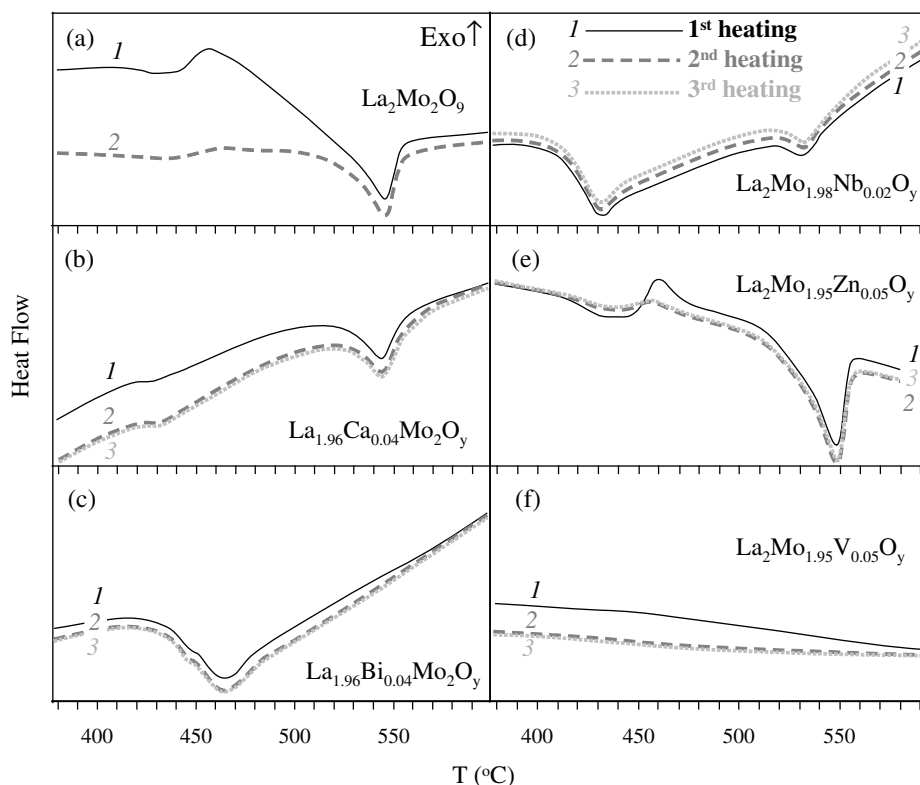Calorimetric characterization of LAMOX single crystals proved rather informative. Figure 5 presents DSC data



**Figure 5.** Calorimetry data for (a) $La_2Mo_2O_9$, (b) $La_{1.96}Ca_{0.04}Mo_2O_y$, (c) $La_{1.96}Bi_{0.04}Mo_2O_y$, (d) $La_2Mo_{1.98}Nb_{0.02}O_y$, (e) $La_2Mo_{1.95}Zn_{0.05}O_y$ and (f) $La_2Mo_{1.95}V_{0.05}O_y$ crystals.
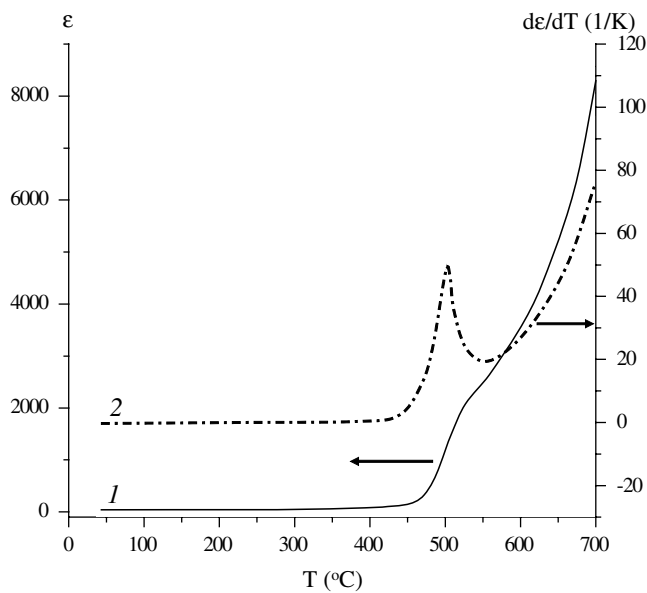
**Figure 6.** (1) Relative dielectric permittivity $\varepsilon$ and (2) its first derivative $d\varepsilon/dT$ as functions of temperature for an $La_{1.96}Bi_{0.04}Mo_2O_y$ single crystal.



**Figure 7.** (1) Calorimetry data and (2) first derivative of the heat flow signal for tungsten-doped LM crystals: (a) $La_2Mo_{1.92}W_{0.08}O_y$, (b) $La_2Mo_{1.84}W_{0.16}O_y$. The third heating stage.

obtained during heating of the quenched crystals. During heating of LM single crystals (figure 5(a)), we observed two endothermic peaks, around 445 and 550 °C. Comparison with our polarization microscopy data indicates that the former peak is the $\beta_{ms} \rightarrow \alpha$ transition, and the latter is the $\alpha \rightarrow \beta$ transition. The $La_{1.96}Ca_{0.04}Mo_2O_y$ crystals (figure 5(b)) also exhibit anomalies due to the $\beta_{ms} \rightarrow \alpha$ and $\alpha \rightarrow \beta$ transitions, near 430 and 545 °C. Earlier, the $\beta_{ms} \rightarrow \alpha$ phase transition in LM doped with 4% Ca was identified directly, using high-temperature XRD [14]: during heating of a metastable cubic sample from 425 to 530 °C, its XRD patterns indicated the cubic to monoclinic phase transition.

The DSC curves of the bismuth-doped LM crystals (figure 5(c)) show two thermal peaks at 445 and 465 °C. The plot of dielectric permittivity versus temperature for the $La_{1.96}Bi_{0.04}Mo_2O_y$ crystal (figure 6) shows a broad peak at 470 and 500 °C, and the temperature derivative of the permittivity has a maximum at 470 °C. It seems likely that $La_{1.96}Bi_{0.04}Mo_2O_y$ undergoes the $\alpha \rightarrow \beta$ phase transition, but its temperature is substantially lower than that in undoped LM crystals.

Figures 5(d)–(f) present DSC data for LM doped with Nb, Zn and V on the Mo site. The DSC curve of the Nb-doped sample, $La_2Mo_{1.98}Nb_{0.02}O_y$, shows two prominent endotherms, in accordance with the report by Basu *et al* [8] that doping with up to 40% Nb does not suppress the $\alpha \rightarrow \beta$ phase transition. In the Zn-doped LM crystals, the intensity of the $\alpha \rightarrow \beta$ endotherm (548 °C) is larger than in LM, whereas the V-doped sample has a cubic structure over the entire temperature range studied (figure 5(f)), as supported by the present polarization microscopy data. Figure 7 illustrates the influence of tungsten content on the thermal behaviour of W-doped LM crystals. In the DSC curve of the sample in which 4% of the Mo is replaced by W, the $\beta_{ms} \rightarrow \alpha$ transition is

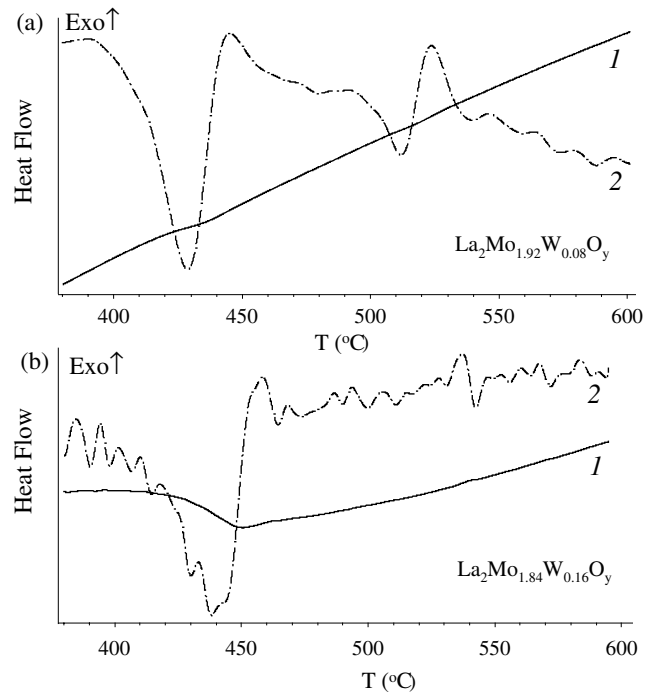well seen (430–440 °C), whereas the $\alpha \rightarrow \beta$ transition is only discernible in the first derivative of the heat flow signal. In the $La_2Mo_{1.84}W_{0.16}O_y$ crystal, which contains twice as much tungsten, the $\alpha \rightarrow \beta$ phase transition cannot be detected even with the use of the first-derivative signal. However, a small event at temperatures near 450 °C is clearly seen. No changes of this thermal event were noted when additional cycles of heating–cooling were performed. Possibly, the process at temperatures near 450 °C taking place in $La_2Mo_{1.84}W_{0.16}O_y$ crystals is connected with oxide ion reorganization but not with the $\beta_{ms} \rightarrow \alpha$ transition. A similar result was obtained for the heavily doped $La_{2-x}Eu_xMo_2O_y$ samples by DTA analysis [17].

## 4. Conclusions

The LAMOX single crystals, undoped and doped with Ca, Bi, Nb, W, V and Zn, were grown by the flux method in the binary system $La_2O_3$–$MoO_3$ and their phase transition peculiarities were investigated by polarization microscopy and calorimetry.

The complex structure of the low-temperature, ordered phase $\alpha$-$La_2Mo_2O_9$ impedes the $\beta \rightarrow \alpha$ phase transition in LM crystals, so that both the $\alpha$-phase and the metastable $\beta_{ms}$-phase (or a mixture of these phases) may exist at room temperature, depending on the post-growth cooling rate and doping level, which was confirmed for the first time by polarization microscopy and calorimetry. The slowly cooled samples had at heating only a $\alpha \rightarrow \beta$ transition. Quenched LAMOX crystals at low doping level undergo the $\beta_{ms} \rightarrow \alpha$ phase transition near 450 °C and the $\alpha \rightarrow \beta$ transition near 550 °C, which can be observed visually, using polarization microscopy, and can be detected by calorimetry

as an endothermic event under heating. At high doping level (for example, $La_2Mo_{1.84}W_{0.16}O_9$) the peak at $450\,°C$ is not associated with the event $\beta_{ms} \rightarrow \alpha$ and it may be the result of defect association/dissociation of oxide ions. The high-temperature $\alpha \rightarrow \beta$ transition disappears at high doping level and crystals have cubic structure over the entire temperature range ($La_2Mo_{1.95}V_{0.05}O_9$ and $La_2Mo_{1.84}W_{0.16}O_9$). So, the phase state and the phase transition sequence of the LAMOX family are determined by the thermal history (heating–cooling rate), the nature of the dopant and the doping level.

## Acknowledgment

## References

[1] Lacorre Ph, Goutenoire F, Bohnke O, Retoux R and Laligant Y 2000 *Nature* **404** 856–8
[2] Yoo K S and Jacobson A J 2005 *J. Mater. Sci.* **40** 4431–4
[3] Goutenoire F, Isnard O, Retoux R and Lacorre Ph 2000 *Chem. Mater.* **12** 2575–80
[4] Malavasi L, Kim H, Billinge S J L, Proffen Th, Tealdi C and Flort G 2007 *J. Am. Chem. Soc.* **129** 6903–7
[5] Evans I R, Howard J A K and Evans J S O 2005 *Chem. Mater.* **17** 4074–7
[6] Voronkova V I, Yanovskii V K and Kharitonova E P 2005 *Crystallogr. Rep.* **50** 874–6
[7] Marozau I P, Marrero-López D, Shaula A L, Kharton V V, Tsipis E V, Núñez P and Frade J R 2004 *Electrochim. Acta* **49** 3517–24
[8] Basu S, Devi P S and Maiti H S 2005 *J. Electrochem. Soc.* **152** A2143–7
[9] Tsai D S, Hsieh M J, Tseng J C and Lee H X J 2005 *J. Eur. Ceram. Soc.* **25** 481–7
[10] Collado J A, Aranda M A G, Cabeza A, Olivera-Pastor P and Bruque S 2002 *J. Solid State Chem.* **167** 80–5
[11] Georges S, Goutenoire F, Lacorre P and Steil M C 2005 *J. Eur. Ceram. Soc.* **25** 3619–27
[12] Li C, Wang X P, Wang J X, Li D, Zhuang Z and Fang Q F 2007 *Mater. Res. Bull.* **42** 1077–84
[13] Marrero-López D, Pérez-Coll D, Ruiz-Morales J C, Canales-Vázquez J, Martin-Sedeño M C and Núñez P 2007 *Electrochim. Acta* **52** 5219–31
[14] Selmi A, Corbel G and Lacorre P 2006 *Solid State Ion.* **177** 3051–5
[15] Hayward S A and Redfern S A T 2004 *J. Phys.: Condens. Matter* **16** 3571–83
[16] Fournier J-P, Fournier J and Kohlmuller R 1970 *Bull. Soc. Chim. Fr.* 4277–83
[17] Corbel G, Chevereau E, Kodjikian S and Lacorre P 2007 *Inorg. Chem.* **46** 6395–404